Physica B 673 (2024) 415438

Contents lists available at ScienceDirect

Physica B: Condensed Matter

journal homepage: www.elsevier.com/locate/physb

Investigating the magneto-transport and thermal properties of 2D electron systems under the influence of the Aharonov–Bohm field and Eckart potential interaction

C.O. Edet [a,b,c], K. Lakaal [d,*], J. El Hamdaoui [d], K. Feddi [e], L.M. Pérez [f], E. Feddi [d,g], A.N. Ikot [h], N. Ali [i,b], Shamsul Amir Abdul Rais [b], M. Asjad [j]

[a] Institute of Engineering Mathematics, Universiti Malaysia Perlis, 02600 Arau, Perlis, Malaysia
[b] Faculty of Electronic Engineering Technology, Universiti Malaysia Perlis, Malaysia
[c] Department of Physics, Cross River University of Technology, Calabar, Nigeria
[d] Group of Optoelectronic of Semiconductors and Nanomaterials, ENSAM, Mohammed V University in Rabat, Rabat 10100, Morocco
[e] Renewable Energy and Advanced Materials Laboratory, International University of Rabat, Morocco
[f] Departamento de Física, FACI, Universidad de Tarapacá, Casilla 7 D, Arica 1000000, Chile
[g] Institute of Applied Physics, Mohammed VI Polytechnic University, Lot 660, Hay Moulay Rachid Ben Guerir 43150, Morocco
[h] Theoretical Physics Group, Department of Physics, University of Port Harcourt, Nigeria
[i] Advanced Communication Engineering (ACE) Centre of Excellence, Universiti Malaysia Perlis, 01000 Kangar, Perlis, Malaysia
[j] Department of Mathematics, Khalifa University, Abu Dhabi 127788, United Arab Emirates

ARTICLE INFO

Keywords:
Schrödinger equation
Eckart potential
Magnetic field
Aharonov–Bohm field

ABSTRACT

The Eckart potential is a well-known potential model with applications cutting across chemical physics and related areas. It is often used to evaluate quantum mechanical tunneling corrections in order to obtain chemical rate constants. To this end, this study focused on extensively examining the effects of perturbations on the magnetic and thermal properties of the Eckart potential. In the presence of magnetic and Aharonov–Bohm fields with Eckart potential, the Schrödinger equation is solved using the functional analysis approach (FAA). The energy equation and wave function are obtained analytically. The energy equation is used to derive expressions for the thermo-magnetic properties of the Eckart potential. An extensive analysis of the effect of these fields and potential parameters on the wave function is presented. In several configurations of the analysis, we observe that the system exhibits a diamagnetic behavior,and the specific heat capacity agree with the Dulong–Petit law. The results of this study are valuable in areas such as molecular physics and condensed matter physics, amongst others.

1. Introduction

In the past decades, many potential functions have been used to model the interactions in a physical system [1–5]. Depending on the nature of the interaction, these potential functions usually have different forms [5–7]. The well-known harmonic oscillator has been applied to study various physical systems over the years. However, recent advances in research have shown that it has some inadequacies. Given this, several improved models have been proposed, such as; Morse potential, Eckart potential, Gaussian potential, etc [8–10]. In order to study these interactions, usually the Schrödinger equation (SE) or any other applicable relativistic equation is solved in the presence of these interaction potentials using numerous mathematical models [3,11–15]. One of the potential models that have been explored extensively is the Eckart potential (EP) (detail is provided in the next section), which is used to carry out many relativistic and non-relativistic quantum mechanical studies [16–30].

Johnston and Heicklen [31] computed the tunneling corrections pertaining to the unsymmetrical Eckart potential within the parameter ranges anticipated for typical chemical reactions occurring at ambient temperatures. Brown [32] showed in his seminal paper a novel approach for the straightforward calculation of tunneling corrections for unsymmetrical Eckart-type potential barriers. Brown [32] (and the references therein) have pointed out that the Eckart potential function is usually used to evaluate quantum mechanical tunneling corrections to chemical rate constants. Considering all these studies, it is necessary

* Corresponding author.
E-mail addresses: collinsokonedet@gmail.com (C.O. Edet), kamal.lakaal@gmail.com (K. Lakaal).

https://doi.org/10.1016/j.physb.2023.415438
Received 16 May 2023; Received in revised form 10 October 2023; Accepted 17 October 2023
Available online 30 October 2023

to evaluate the temperature- and magnetism-related effects (Aharonov–Bohm (AB) and magnetic fields) on thermal and magnetic properties of the Eckart potential.

Numerous studies have demonstrated the importance of the role played by effects such as; Rashba, Dresslhauss or Zeeman in modifying the behavior of many quantum systems [33–37]. Amongst those effects, eliminating degeneracy with magnetic field is one of the most significant and most studied in literature [38]. The same statement can be said about when a system is placed in the Aharonov–Bohm (AB) field [38–42]. The study of the effects of those perturbations is widely investigated in the literature [9,12,33,43–45]. In the presence of Aharonov–Bohm and position-dependent external magnetic fields, the paper published by Edet et al. [46] provided the solutions of the position-dependent mass Schrödinger equation (PDMSE) for the screened Kratzer potential.Edet and Ikot [47] team used the Hulten–Kratzer potential (HKP) model to conduct a study on the N_2, I_2, CO, NO and HCl diatomic molecules in the presence of AB and magnetic fields. Continuing in the same direction as those two papers, the main goal of this study is to examine the effects external field perturbation has on the thermodynamic and magnetic properties of the Eckart potential.

The present study is focused on the solutions of 2D Schrödinger equation taking into consideration perturbations, using the Eckart potential as the interaction potential. This analytical solution will be achieved using the functional analysis approach (FAA). To this end, the eigensolutions (wave function and energy equation) will be obtained, taking into account the effects of the perturbations. Using the obtained energy, both thermal and magnetic properties will be evaluated.

The present study is structured as follows; Section 2 of the paper outlines the solutions of the Schrödinger equation with the Eckart potential. Section 3 will provide a detailed derivation of the partition function, as well as an analysis and discussion of the magnetic and thermal properties of the system. Section 4 of the document comprises the presentation of conclusion and a discussion of potential future developments.

2. Non-relativistic model and solutions

Assuming polar coordinates (r, φ), the Hamiltonian for a non-relativistic system that is subject to the Eckart potential $V(r)$ and the influence of an applied external magnetic field and AB flux can be expressed as per various studies [42,47,48].

$$\left[\frac{1}{2\mu}\vec{p}^2 + V(r)\right]\psi(r,\varphi) = E\psi(r,\varphi), \tag{1}$$

where E is the energy eigenvalues, μ represents the effective mass of the system and $V(r) = -\upsilon_1\mathcal{V}_1(r) + \upsilon_2\mathcal{V}_2(r)$ is the Eckart potential with υ_1 and υ_2 are two adjustable potential parameters. Here, $\mathcal{V}_1(r) = e^{-\alpha r}/(1-e^{-\alpha r})$ and $\mathcal{V}_2(r) = \mathcal{V}_1(r)/(1-e^{-\alpha r})$, where α is the screening parameter and r is the inter-nuclear distance [16,17,49]. The following is an investigation of the physical process under the effect of EP $V(r)$. Under such conditions, the momentum operator of the particle has to change. To achieve that, we minimally couple a four-vector to the momentum operator given by $\vec{p} = i\hbar\vec{\nabla} + \frac{q}{c}\vec{A}$. In order to take into consideration both the AB flux and magnetic field together, the vector total vector potential $\vec{A}$ is expressed as a superposition of two vector potential terms as $\vec{A} = \vec{A}_1(r) + \vec{A}_2(r)$ where $\vec{A}_1 = Be^{-\alpha r}\widehat{\varphi}/(1-e^{-\alpha r})$ and $\vec{A}_2 = (1/2\pi r)\phi_{AB}\widehat{\varphi}$. Here, B represents the magnetic field, and ϕ_{AB} is the AB flux. The two vector potentials $\vec{A}_1(r)$ and $\vec{A}_2(r)$ also satisfied $\vec{\nabla}\wedge\vec{A}_1(r) = \vec{B}$ and $\vec{\nabla}.\vec{A}_1(r) = 0$.

To solve of the stationary SE in Eq. (1), we make ansatz

$$\psi(r,\varphi) = \frac{1}{\sqrt{2\pi r}}e^{im\varphi}P_{nm}(r), \tag{2}$$

Here, m is the magnetic quantum number. When the above ansatz is inserted in Eq. (1), the radial equation takes the form of:

$$P''_{nm}(r) + \frac{2\mu}{\hbar^2}\left[E_{nm} - V_{eff}(r,\omega_c,\xi)\right]P_{nm}(r) = 0, \tag{3}$$

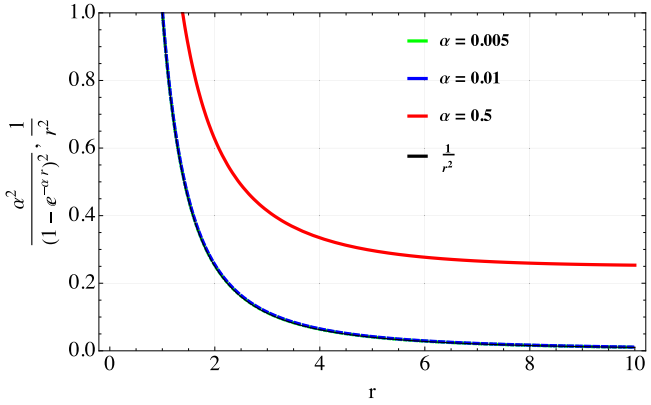

Fig. 1. Plot of centrifugal term $1/r^2$ (black curve) and its approximation $\alpha^2/(1-e^{-\alpha r})^2$ with r for different α values ($\alpha = 0.005$ (green curve), 0.01 (blue curve), and 0.5 (red curve)).

where the effective potential $V_{eff}(r,\omega_c,\xi)$, is defined as follows:

$$V_{eff}(r) = -\upsilon_1\mathcal{V}_1(r) + \upsilon_2\mathcal{V}_2(r) + \frac{\hbar\omega_c(m+\xi)}{r}\mathcal{V}_1(r) + \frac{\mu\omega_c^2}{2}\mathcal{V}_1^2(r) + \frac{\hbar^2}{2\mu r^2}\left[(m+\xi)^2 - \frac{1}{4}\right], \tag{4}$$

$\omega_c = \frac{eB}{\mu c}$ is the cyclotron frequency and $\xi = \frac{\phi_{AB}}{\phi_0}$ represents an integer with the flux quantum $\phi_0 = \frac{hc}{e}$. Since the presence of the centrifugal term in the effective potential does not allow us to achieve an analytical solution for Eq. (3), the use of the Greene and Aldrich approximation scheme [46,47] that is only valid for small values of the screening parameter becomes indispensable to bypass the centrifugal term.

$$\frac{1}{r^2} \approx \frac{\alpha^2}{(1-e^{-\alpha r})^2} \tag{5}$$

As shown in Fig. 1, it is explicitly clear that when α is large, say $\alpha = 0.5$, the approximation is not fit to approximate the barrier. On the other hand, there is an obvious overlap and fit of the approximation and the barrier when α is very small, say $\alpha = 0.005$ and $\alpha = 0.01$, as depicted in Fig. 1. Now by introducing a new variable $s = e^{-\alpha r}$, and rewriting the Eq. (3) in terms of the s, one gets

$$\frac{d^2P_{nm}(s)}{ds^2} + \frac{1}{s}\frac{dP_{nm}(s)}{ds} - \frac{\mathcal{U}_0 s^2 + \mathcal{U}_1 s + \mathcal{U}_2}{s^2(1-s)^2}P_{nm}(s), \tag{6}$$

where $\mathcal{U}_0 = \varepsilon - \tau_0 + \tau_3$, $\mathcal{U}_1 = 2\varepsilon + \tau_0 - \tau_1 - \tau_2$ and $\mathcal{U}_2 = \varepsilon + \tau_4$ with $\varepsilon = 2\mu E/(\hbar^2\alpha^2)$, $\tau_0 = 2\mu\upsilon_1/(\hbar^2\alpha^2)$, $\tau_1 = 2\mu\upsilon_2/(\hbar^2\alpha^2)$, $\tau_2 = 2\mu\omega_c(m+\xi)/(\hbar\alpha)$, $\tau_3 = \mu^2\omega_c^2/(\hbar^2\alpha^2)$ and $\tau_4 = (m+\xi)^2 - 1/4$.

To solve Eq. (6), it is necessary to convert the equation into a form that can be solved using a standard mathematical technique. For the purpose of this study, the functional analysis method is employed. The differential equation (Eq. (6)) has two regular singularities at s = 0 and 1 [50] so that it can be reduced to the hypergeometric equation by substituting

$$P_{nm}(s) = s^{\lambda}(1-s)^{\eta}f_{nm}(s), \tag{7}$$

where $\lambda = \sqrt{\varepsilon+\tau_4}$ and $\eta = \frac{1}{2} + \sqrt{\frac{1}{4}+\tau_1+\tau_2+\tau_3+\tau_4}$. Now, by substituting Eq. (7) in Eq. (6), the hypergeometric differential equation can be derived as follows:

$$s(1-s)f''_{nm}(s) + \left[2\lambda + 1 + 2(\lambda+\eta+1/2)s\right]f'_{nm}(s) - \left[(\lambda+\eta)^2 - \mathcal{U}_0\right]f_{nm}(s) = 0. \tag{8}$$

Then the solutions of Eq. (8) are the hypergeometric functions ${}_2F_1(a,b;c;s)$, where $a = \lambda+\eta+\sqrt{\mathcal{U}_0}$, $b = \lambda+\eta-\sqrt{\mathcal{U}_0}$, and $c = 2\lambda+1$. According to the hypergeometric function properties, this series $f_{nm}(s)$ given in the above equation approaches infinity unless $a = \lambda+\eta-\sqrt{\mathcal{U}_0}$

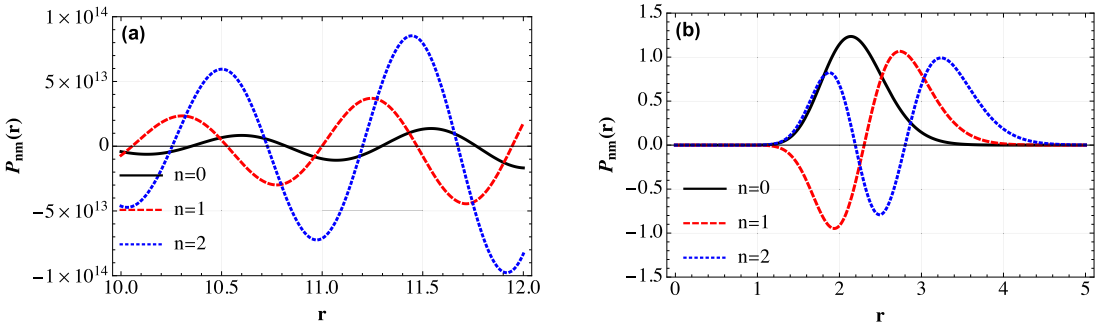

Fig. 2. **(a)** Wave function of EP with r in the presence of $\vec{B}$ and ξ; **(b)** in the presence of magnetic field ($\vec{B} \neq 0$) and absence of AB field ($\xi = 0$).

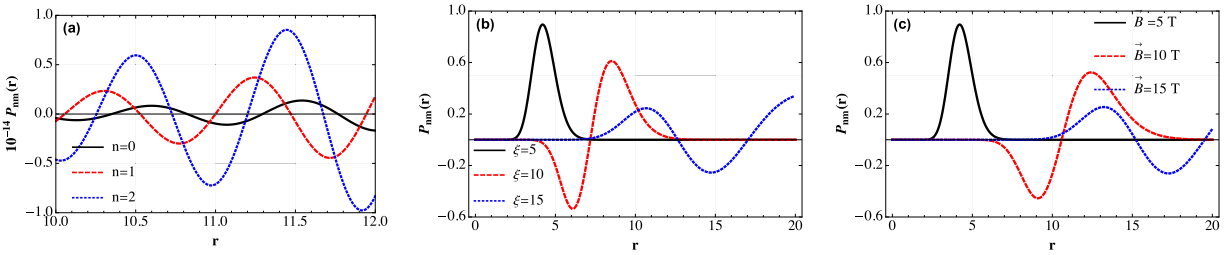

Fig. 3. **(a)** Wave function of EP with r in the case of $B = 0$ and $\xi \neq 0$; **(b)** varying AB field and fixed Magnetic field for $n = 0$. (c) Wave function of EP with r with varying B and fixed value of AB field for $n = 0$.

is a negative integer [50]. ${}_2F_1(a, b; c; s)$, From the above equation, we can give more insight into the solutions. The boundary condition areas are;

$$f_{nm}(s)|_{s=0} = 0$$
$$f_{nm}(s)|_{s=1} = 0 \tag{9}$$

The solutions of Eq. (7) are as follows:

$$P_{nm}(s) = s^{\lambda}(1-s)A\ {}_2F_1\left(\lambda+\eta+\sqrt{U_0}, \lambda+\eta-\sqrt{U_0}, 2\lambda+1; s\right) + s^{2\lambda}B\ {}_2F_1\left(-\lambda+\eta+\sqrt{U_0}, -\lambda+\eta-\sqrt{U_0}, -2\lambda+1; s\right) \tag{10}$$

where A and B are constant coefficients. The value of B is zero using the 1st boundary condition in Eq. , $B = 0$. Now to consider the 2nd boundary condition in Eq. , we expand the hypergeometric function ${}_2F_1(a, b, c; s)$ near $s = 1$, this details are provided in Lebedev [51] and Setare and Karimi [52]. Therefore, the radial wave function $P(s)$ will not be finite everywhere unless $\lambda + \eta - \sqrt{U_0} = -n$ (for n=0,1,2,..). The functional analysis approach is also known as the factorization method. Details of the method can be found in Ref. [53]. Therefore, we obtain the radial wave function as follows:

$$P_{nm}(s) = N_{nm}s^{\lambda}(1-s)^{\eta}{}_2F_1(a, b, c; s) \tag{11}$$

Here, N_{nm} is the normalization constant, and in the presence of AB and magnetic fields, the energy eigenvalue E of the Eckart potential is given by

$$E = \frac{\hbar^2\alpha^2}{2\mu}\tau_4 - \frac{\hbar^2\alpha^2}{8\mu}\left(\frac{\tau_1+\tau_3-\tau_4-(n+\eta)^2}{n+\eta}\right), \tag{12}$$

The ground, first, and second excited state wave functions of the EP are displayed in Figs. 2 and 3 as a function of r for different magnetic and AB fields. As the quantum number increases, the nodes become more distinct, and the same trend is observed for all the cases investigated.

3. Thermo-magnetic properties

The canonical partition function $Z(\beta)$ provides a measure of the thermally accessible states and is introduced to analyze the thermodynamic and magnetic properties of the EP at a limited temperature T. It can be determined by summing up all energy states. The Boltzmann–Gibbs distribution gives the expression for $Z(\beta)$, which is given by [4, 54,55]

$$Z(\beta) = \sum_{n=0}^{n_{\max}} e^{-\beta E_n} \tag{13}$$

where $\beta = \frac{1}{kT}$ and with k is the Boltzmann constant. Substituting Eq. (12) in Eq. (13), we get

$$Z(\beta) = \sum_{n=0}^{n_{\max}} e^{-\beta\left(z_0 - z_2\left(\frac{z_1-(n+\widetilde{\sigma})^2}{(n+\widetilde{\sigma})}\right)^2\right)} \tag{14}$$

where the variable n represents the vibrational quantum number, which takes on integer values from 0 to $n_{\max}$, where $n_{\max}$ is the maximum vibrational quantum number allowed. Here $z_0 = \hbar^2\alpha^2\tau_4/2\mu$, $z_1 = \tau_0 + \tau_3 - \tau_4$ and $z_2 = \hbar^2\alpha^2/8\mu$. By substituting the summation with an integral in Eq. (14), we obtain:

$$Z(\beta) = \int_0^{n_{\max}} e^{-\beta\left(z_0 - z_2\left(\frac{z_1-(n+\widetilde{\sigma})^2}{(n+\widetilde{\sigma})}\right)^2\right)} dn. \tag{15}$$

If we define ω as $n + \eta$, we can express the integral in Eq. (15) in the following manner:

$$Z(\beta) = \int_{x_1}^{x_2} e^{\beta\left(\frac{z_1 z_2^2}{\omega^2} + z_2\omega + z_3\right)} d\omega, \tag{16}$$

where $x_1 = \eta$, $x_2 = n_{\max} + \eta$ and $z_3 = -2z_2z_1 - z_0$. After solving the integral presented in Eq. (16), we derive the partition function of the EP under AB and magnetic fields, which is given by:

$$Z(\beta) = \frac{\sqrt{\pi}e^{-z_0\beta}}{4\sqrt{-z_2\beta}}\left\{\Xi_1 + e^{4z_1z_2\beta}\mathrm{Erf}\left[x_1\mathrm{Erf}[\sqrt{-z_2\beta}] - \sqrt{z_1^2z_2\beta}/x_1\right]\right\} + \frac{\sqrt{\pi}e^{-z_0\beta}}{4\sqrt{-z_2\beta}}\left\{-\Xi_2 - e^{4z_1z_2\beta}\mathrm{Erf}\left[x_2\mathrm{Erf}[\sqrt{-z_2\beta}] - \sqrt{z_1^2z_2\beta}/x_2\right]\right\} \tag{17}$$

where $\Xi_{1,2} = \mathrm{Erf}\left[x_{1,2}\sqrt{-z_2\beta}\right] - \sqrt{z_1^2z_2\beta}/x_{1,2}$. The above equation is the classical partition function, as it does not include any quantum corrections, as noted in Eq. (17). In the subsequent subsection, we use the partition function Eq. (17), $Z(\beta)$, to derive all thermodynamic and

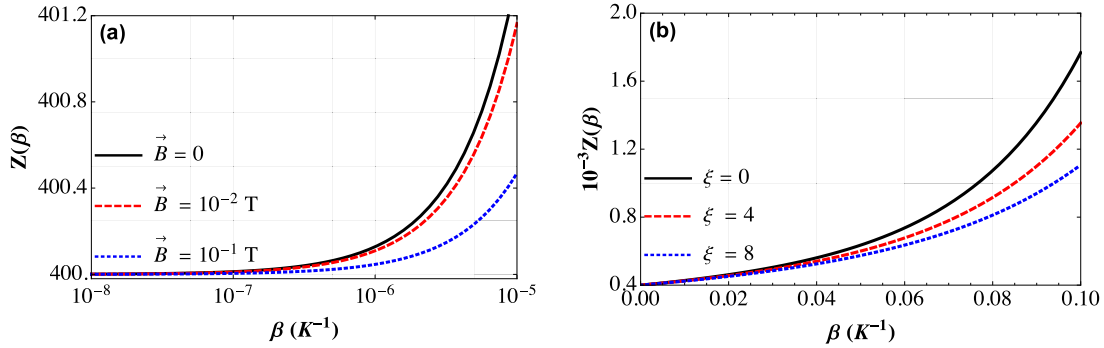

Fig. 4. Variation of $Z(\beta)$ with respect to β, **(a)** with various magnetic and **(b)** with various AB fields.

$$U(\beta)=\frac{-\sqrt{-z_2\beta}4e^{2z_1z_2\beta}(x_1e^{x_2x_1^{-1}(x_1^4+z_1^2)\beta}-x_2e^{x_2x_2^{-1}(x_1^4+z_1^2)\beta})+\sqrt{\pi}[\Xi_1(S_+-e^{4z_1z_2\beta}S_-)+\Xi_2(S_++e^{4z_1z_2\beta}S_-)]}{2\sqrt{\pi}\beta\left(-1+\Xi_1+e^{z_1z_2\beta}(\Xi_1-\Xi_2)+\Xi_{c2}\right)}, \tag{18}$$

Box I.

magnetic properties of the EP subjected to magnetic and AB fields. These properties include free energy, specific heat, entropy, mean energy, magnetic susceptibility, magnetization, and persistent current. We can calculate these thermodynamic functions of the EP using the following expressions [13,42,46,55].

Fig. 4 illustrates the partition function $Z(\beta)$ as a function of β for various magnetic field values ($B=0$, $B=10^{-2}$ and $B=10^{-1}$T) in Fig. 4(a), and different AB field values ($\xi=0$, $\xi=4$, and $\xi=8$) in Fig. 4(b). The Fig. 4(a) shows that, the partition function remains invariant when the magnetic field is zero. However, when a magnetic field is introduced with a fixed AB field, $Z(\beta)$ decreases as the temperature rises. Fig. 4(b) illustrates $Z(\beta)$ variation with temperature and AB field while keeping the magnetic field constant. It is shown that as temperature and AB field increase, the partition function also increases.

3.1. Thermodynamic functions

The magnetic and thermal properties of the Eckart potential are examined under three scenarios: (1) investigating the behavior of all the magnetic and thermal properties as magnetic field and temperature change while the AB field is kept constant, (2) exploring the behavior of all the magnetic and thermal properties as AB field and temperature vary while the magnetic field is fixed, and (3) studying the magnetic properties as magnetic and temperature field vary while the AB field is fixed, and vice versa for both zero and finite values. temperatures.

Internal energy. The internal energy $U(\beta)=-\frac{d\ln Z(\beta)}{d\beta}$ of the system, given that the volume is constant, can be expressed as in Box I [56,57]: where $\Xi_{c1,2}=\mathrm{Erfc}\left[x_{1,2}\sqrt{-z_2\beta}\right]-\frac{\sqrt{-z_1^2z_2\beta}}{x_{1,2}}$ and $S_\pm=1-2z_3\beta\pm4z_1^2z_2\beta$.

Fig. 5 shows $U(\beta)$ plotted against the temperature for different magnetic field Fig. 5(a) and static AB field Fig. 5(b). $U(\beta)$ depreciates with rising temperature. The internal energy is high for low or absence of $\vec{B}$. The internal energy of the system is shown to decrease with temperature and decrease with rising AB field in Fig. 5(b).

Free energy. The free energy associated with the Eckart potential is defined as $F(\beta)=-\frac{1}{\beta}\ln Z(\beta)$, where $Z(\beta)$ is the partition function [56,57]. Fig. 6(a) depicts that when the magnetic field is absent and the AB field is fixed, the free energy rises monotonically as the temperature increases. However, in the presence of a magnetic field, the free energy does not display a clear trend. Nevertheless, the free energy is higher for lower magnetic fields. Fig. 6(b) illustrates the variation of the free energy with increasing temperature and AB field. The free energy exhibits a monotonically increasing trend with temperature, and the AB field has a stronger impact on the free energy at lower values. This finding is consistent with our previous observation regarding the impact of the magnetic field on the free energy, as shown in Fig. 6(a).

Entropy. The entropy, denoted as $S(\beta)$, is an essential thermodynamic property that measures the level of disorder or randomness in the system. Its value can be obtained using the formula $S=\ln Z(\beta)-\beta\frac{d\ln Z(\beta)}{d\beta}$ [56,57]. In Fig. 7(a), the entropy is plotted against varying β and magnetic field while keeping the AB field constant. The plot reveals that the entropy declines as the temperature rises, and the entropy reduces for a higher magnetic field. Fig. 7(b) illustrates how the entropy changes with increasing temperature and AB field, indicating that the entropy declines as the AB field and temperature increase.

Heat capacity. The relation $C(\beta)=\beta^2\frac{d^2\ln Z(\beta)}{d\beta^2}$ defines the specific heat $C(\beta)$ of the system, which tells us how much energy can be stored per unit temperature increase [56,57]. In Fig. 8(a), the specific heat capacity is plotted versus temperature for different magnetic field. The figure clearly indicates that the specific heat capacity $C(\beta)$ increases as the temperature rises, which is consistent with the Dulong–Petit law [9,55]. Additionally, Fig. 8(b) shows the change in $C(\beta)$ with increasing AB field and temperature. The specific heat capacity is observed to increase with increasing temperature and AB field in Fig. 8(b), which is in agreement with the Dulong–Petit law.

3.2. Magnetic properties at $T\neq0$

This section presents a discussion on the various magnetic properties exhibited by the Eckart potential at non-zero temperatures.

Magnetization $M(\beta)$. The statistical relation can be utilized to extract the magnetization $M(\beta)$.

$$M(\beta)=\frac{1}{\beta}\left(\frac{1}{Z(\beta)}\right)\left(\frac{\partial}{\partial\vec{B}}Z(\beta)\right), \tag{19}$$

Fig. 9(a) displays the plot of magnetization $M(\beta)$ as a function of temperature for different $\vec{B}$. The magnetization increases with increasing temperature and decreases with increasing $\vec{B}$. Magnetization versus temperature for different AB field is shown in Fig. 9(b). The magnetization rises with rising temperature and AB field. The magnetization $M(\beta)$ as a function of the magnetic field $\vec{B}$ is shown in Fig. 10(a).

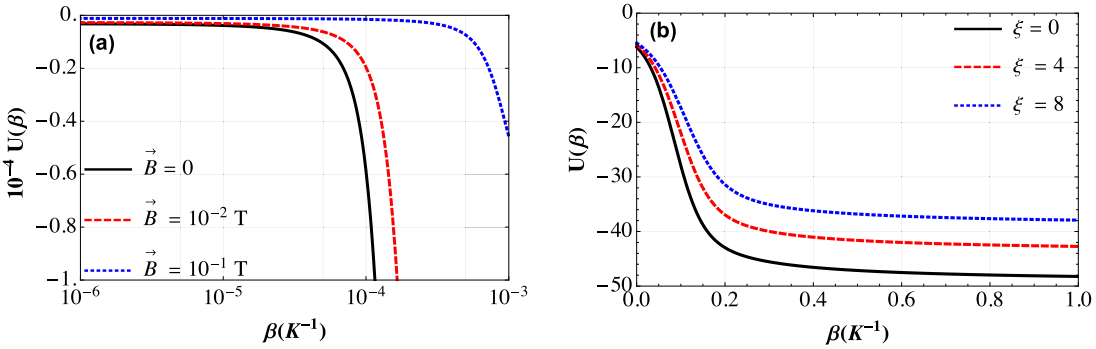

Fig. 5. **(a)** plot the internal energy $U(\beta)$ against β for different magnetic field values, **(b)** $U(\beta)$ against β for different AB field values.

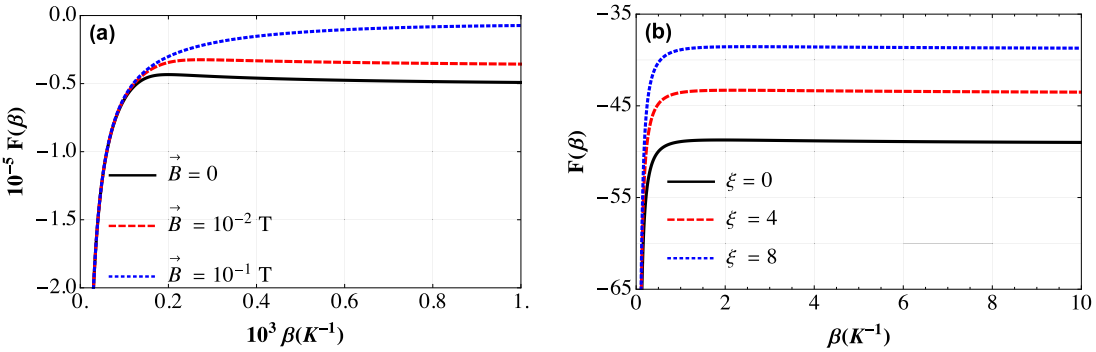

Fig. 6. Plot the Free energy against β, **(a)** for different magnetic field values, **(b)** for different AB field values.

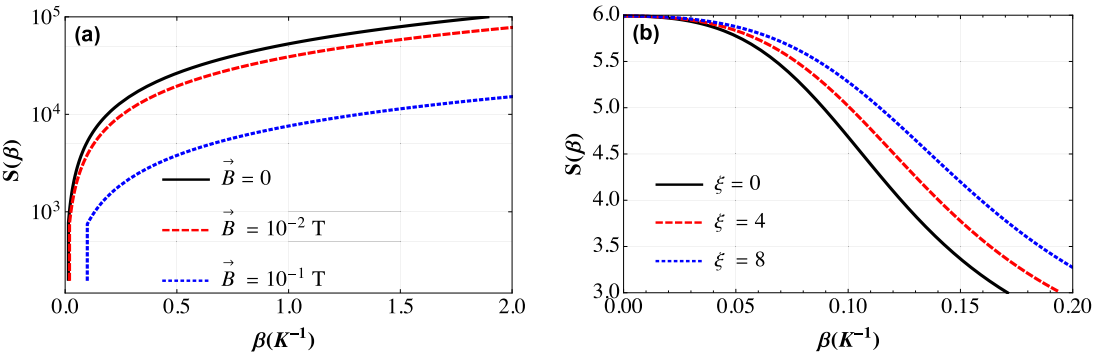

Fig. 7. Plot the entropy against β, **(a)** for different magnetic field values, **(b)** for different AB field values.

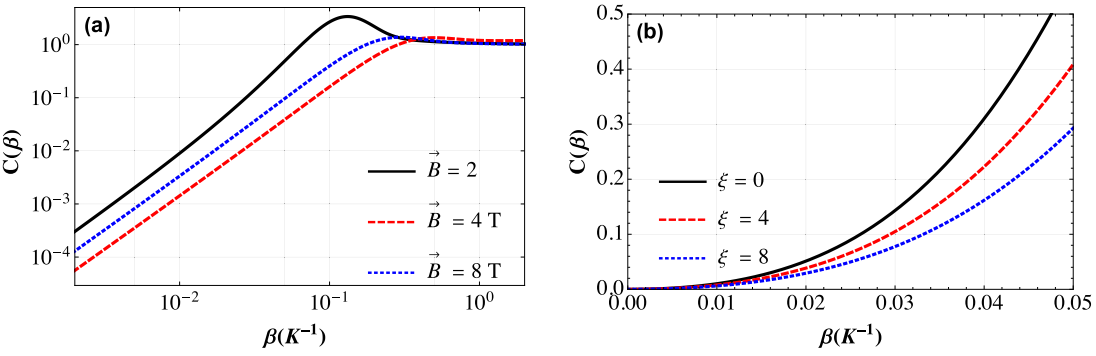

Fig. 8. Plot the heat capacity against β, **(a)** for different magnetic field values, **(b)** for different AB field values.

The magnetization decreases as $\vec{B}$ increases, and it is less affected by temperature variations, with a monotonous increase observed at zero temperature. Fig. 10(b) shows that $M(\beta)$ rises with AB field at zero temperature, but at finite temperatures, it shows a quasi-invariant trend as the AB field varies. The magnetization is more sensitive to temperature variations.

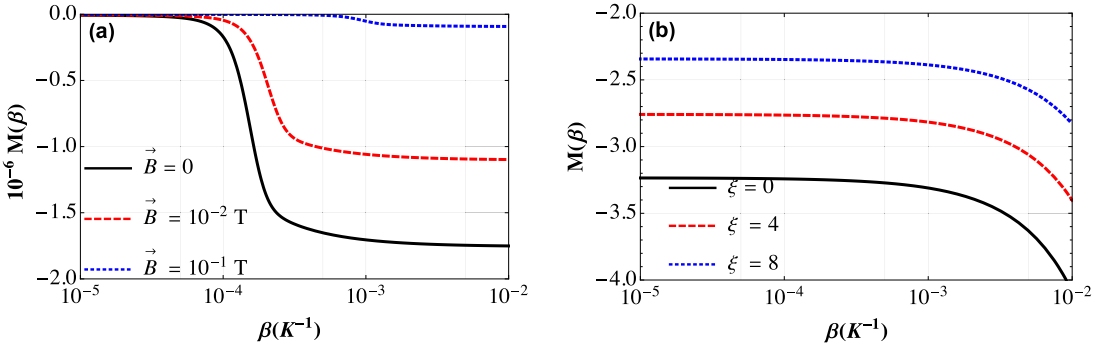

Fig. 9. Plot of Magnetization against β, **(a)** for different magnetic field values, **(b)** for different AB field values.

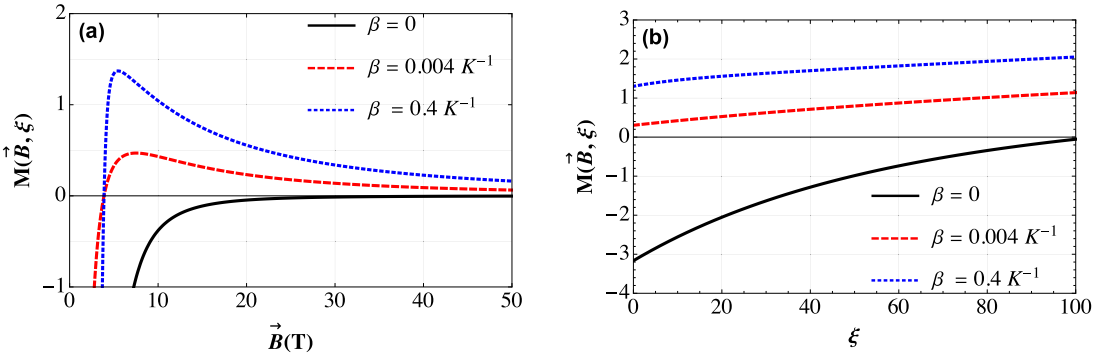

Fig. 10. Plot of Magnetization against **(a)** Magnetic and **(b)** AB Fields varying β.

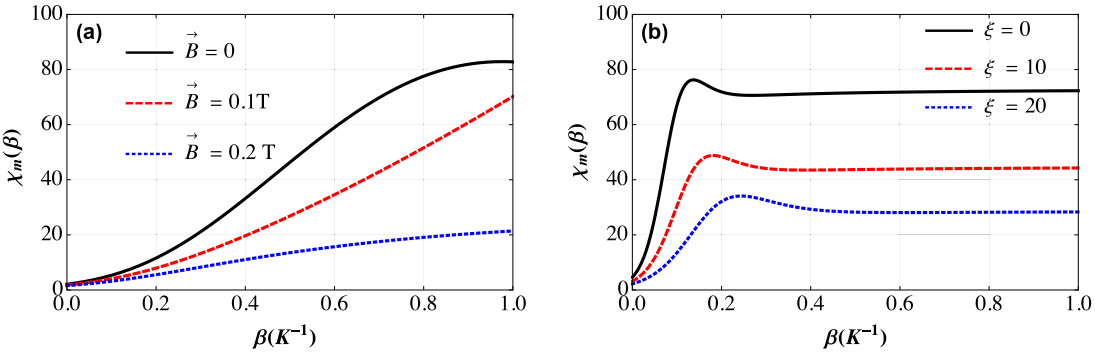

Fig. 11. Plot of Magnetic Susceptibility against β, **(a)** for different magnetic field values, **(b)** for different AB field values.

Magnetic susceptibility $\chi(\beta)$. It is worth noting that the assessment of the magnetization degree of a particular material subjected to a magnetic field (B) can be established through the magnetic susceptibility, as follows:

$$\chi(\beta) = \frac{\partial M(\beta)}{\partial \vec{B}} \tag{20}$$

Fig. 7(a) illustrates the relation between magnetic susceptibility and temperature under different magnetic fields. The magnetic susceptibility increases and peaks at $0.2K^{-1}$ and rises swiftly as the temperature upsurges. In Fig. 11(b), $\chi(\beta)$ versus temperature and the varying AB field. Again, the susceptibility first peaks and the decreases with rising temperature.

As shown in Fig. 12(a), the magnetic susceptibility at $T \neq 0$ is insensitive to the presence of $\vec{B}$ and temperature variation. At $T = 0$, the magnetic susceptibility decreases to a minimum in the neighborhood of $\vec{B} = 1T$ and rises again as the magnetic rises. Again, in Fig. 12(b), $\chi(\beta)$ is insensitive to the varying AB field and temperature variation. At $T = 0$, the susceptibility increase with rising AB field in a similar way like what was observed earlier in the presence of different $\vec{B}$.

Persistent current $I(\beta)$. Finally the persistent current $I(\beta)$ can be calculated using the expression $I(\beta) = -\frac{\partial F(\beta)}{\partial \phi_{AB}}$.

Fig. 13(a) displays the persistent current variation with $\vec{B}$ and temperature. The persistent current increases in a quasi-monotonic behavior with increasing magnetic field and temperature. By inspection, it can be inferred that the magnetic susceptibility, internal energy, entropy, persistent current and specific heat capacity are not sensitivity to the presence of $\vec{B}$. The graph depicted in Fig. 13(b) displays a monotonic decrease of the persistent current as the temperature increases. The persistent current is more prominent at higher AB field values.

The plot in Fig. 14(a) demonstrates a continuous increase in the persistent current as the magnetic field increases at zero temperature. At $T \neq 0$, the persistent current increase with rising $\vec{B}$ but suddenly drops at $\vec{B} = 60T$ for $\beta = 0.8K^{-1}$. Fig. 14(b) shows the persistent current against AB field with varying temperatures. At zero temperature, it is shown that the persistent current rises in a monotonic pattern with

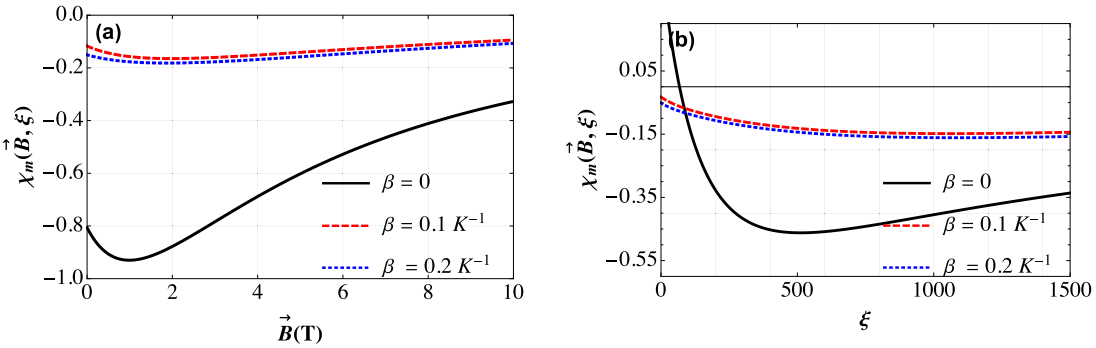

Fig. 12. Plot of Magnetic Susceptibility against **(a)** Magnetic and **(b)** AB Fields varying β.

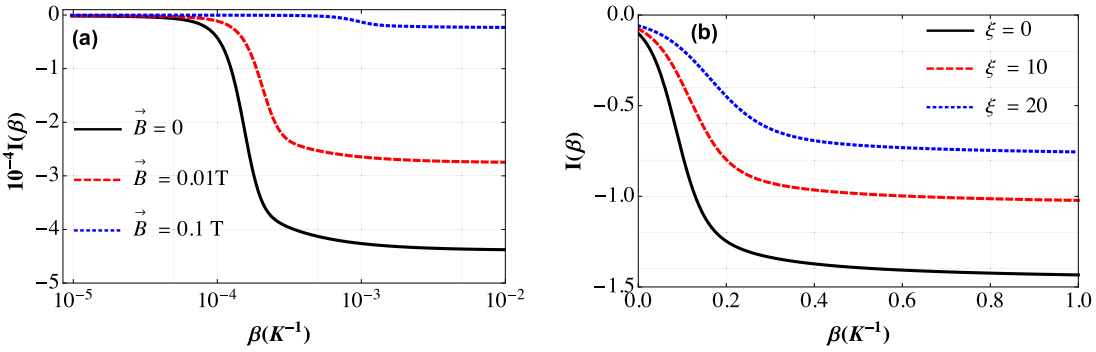

Fig. 13. Plot of Persistent Current against β, **(a)** for different magnetic field values, **(b)** for different AB field values.

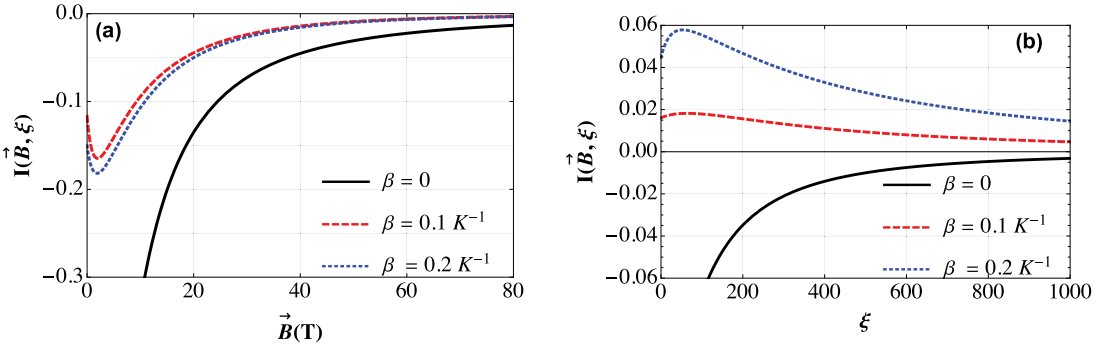

Fig. 14. **(a)** Plot of Persistent Current with $\vec{B}(T)$ varying β, **(b)** Variation of Persistent Current with Respect to ξ varying β.

increasing AB field. At $T \neq 0$, the persistent current drops linearly with increasing AB field, and there exists a spacing between the representative curves, indicating some level of sensitivity to the AB field and temperature.

4. Conclusion

This study investigates the magnetic and thermal properties of the Eckart potential in the presence of Aharonov–Bohm and magnetic fields. The FAA method is utilized to solve the Schrödinger equation, resulting in an energy spectrum and wave function that is approximate-analytic and expressed in hypergeometric functions. Analytic expressions for the thermo-magnetic properties are then derived from the energy equation. Graphical analyses have been presented to demonstrate the impact of perturbations on the thermo-magnetic characteristics. Additionally, an analysis is conducted on the influence of these fields on the wave functions. The present study emphasizes the system's high sensitivity to the magnetic field. The obtained analytical expressions can be used to investigate other physical systems by adjusting the potential parameters, thereby expanding the frontiers of knowledge. The findings of this study have practical implications in various fields, such as atomic physics, condensed matter physics, chemical physics, and related disciplines.

Funding

This research has been carried out under the Long Term Research Grant Scheme (LRGS) with grant number LRGS/1/2020/UM/01/5/2 (9012-00009) provided by the Ministry of Higher Education of Malaysia (MOHE).

CRediT authorship contribution statement

C.O. Edet: Conceptualization, Methodology, Formal analysis, Investigation, Writing – original draft. **K. Lakaal:** Conceptualization, Methodology, Formal analysis, Investigation, Writing – original draft. **J. El Hamdaoui:** Conceptualization, Methodology, Formal analysis, Investigation, Writing – original draft. **K. Feddi:** Conceptualization,

Writing – review & editing, Supervision, Project administration. **L.M. Pérez:** Conceptualization, Writing – review & editing, Supervision, Project administration. **E. Feddi:** Conceptualization, Writing – review & editing, Supervision, Project administration. **A.N. Ikot:** Conceptualization, Writing – review & editing, Supervision, Project administration. **N. Ali:** Conceptualization, Writing – review & editing, Supervision, Project administration. **Shamsul Amir Abdul Rais:** Conceptualization, Writing – review & editing, Supervision, Project administration. **M. Asjad:** Conceptualization, Writing – review & editing, Supervision, Project administration.

Declaration of competing interest

The authors confirm that they do not have any conflict of interest in connection with this investigation.

Data availability

No data was used for the research described in the article.

Acknowledgments

L.M.P. acknowledges financial support from the ANID through Convocatoria Nacional Subvención a Instalación en la Academia Convocatoria Año 2021, Grant SA77210040.

References

[1] C.-S. Jia, Y. Li, Y. Sun, J.-Y. Liu, L.-T. Sun, Phys. Lett. A 311 (2003) 115.
[2] C.-S. Jia, T. Chen, L.-G. Cui, Phys. Lett. A 373 (2009) 1621.
[3] C.-S. Jia, T. Chen, S. He, Phys. Lett. A 377 (2013) 682.
[4] C.-S. Jia, C.-W. Wang, L.-H. Zhang, X.-L. Peng, R. Zeng, X.-T. You, Chem. Phys. Lett. 676 (2017) 150.
[5] U.S. Okorie, E.E. Ibekwe, A.N. Ikot, M.C. Onyeaju, E.O. Chukwuocha, J. Korean Phys. Soc. 73 (2018) 1211.
[6] S.-H. Dong, M. Cruz-Irisson, J. Math. Chem. 50 (2012) 881.
[7] C.O. Edet, P.O. Okoi, Rev. Mex. Física 65 (2019) 333.
[8] R. Khordad, B. Mirhosseini, Pramana 85 (2015) 723.
[9] M. Servatkhah, R. Khordad, A. Firoozi, H.R. Rastegar Sedehi, A. Mohammadi, Eur. Phys. J. B 93 (2020) 1.
[10] G.-D. Zhang, J.-Y. Liu, L.-H. Zhang, W. Zhou, C.-S. Jia, Phys. Rev. A 86 (2012) 062510.
[11] M. Abu-Shady, C.O. Edet, A.N. Ikot, Can. J. Phys. 99 (2021) 1024.
[12] S.M. Ikhdair, R. Sever, Adv. High Energy Phys. 2013 (2013).
[13] A.N. Ikot, E.O. Chukwuocha, M.C. Onyeaju, C.A. Onate, B.I. Ita, M.E. Udoh, Pramana 90 (2018) 1.
[14] A.N. Ikot, U.S. Okorie, G.J. Rampho, P.O. Amadi, C.O. Edet, I.O. Akpan, H.Y. Abdullah, R. Horchani, J. Low Temp. Phys. 202 (2021) 269.
[15] C.-S. Jia, Y. Jia, Eur. Phys. J. D 71 (2017) 1.
[16] C.O. Edet, U.S. Okorie, G. Osobonye, A.N. Ikot, G.J. Rampho, R. Sever, J. Math. Chem. 58 (2020) 989.
[17] B.J. Falaye, Cent. Eur. J. Phys. 10 (2012) 960.
[18] S.-H. Dong, W.-C. Qiang, G.-H. Sun, V.B. Bezerra, J. Phys. Math. Theor. 40 (2007) 10535.
[19] H. Goudarzi, V. Vahidi, Adv. Stud. Theor. Phys. 5 (2011) 469.
[20] C.-S. Jia, P. Guo, X.-L. Peng, J. Phys. Math. Gen. 39 (2006) 7737.
[21] X.-Y. Liu, G.-F. Wei, C.-Y. Long, Internat. J. Theoret. Phys. 48 (2009) 463.
[22] D. Nath, A.K. Roy, Chem. Phys. Lett. 780 (2021) 138909.
[23] E. Olgar, R. Koç, H. Tütüncüler, Chin. Phys. Lett. 23 (2006) 539.
[24] C.P. Onyenegecha, U.M. Ukewuihe, A.I. Opara, C.B. Agbakwuru, C.J. Okereke, N.R. Ugochukwu, S.A. Okolie, I.J. Njoku, Eur. Phys. J. Plus 135 (2020) 1.
[25] R.A. Sari, A. Suparmi, C. Cari, Chin. Phys. B 25 (2015) 010301.
[26] A. Soylu, O. Bayrak, I. Boztosun, J. Phys. Math. Theor. 41 (2008) 065308.
[27] F. Taskin, G. Koçak, Chin. Phys. B 19 (2010) 090314.
[28] G.-F. Wei, S.-H. Dong, V.B. Bezerra, Internat. J. Modern Phys. A 24 (2009) 161.
[29] L.-H. Zhang, X.-P. Li, C.-S. Jia, Phys. Lett. A 372 (2008) 2201.
[30] X. Zou, L.-Z. Yi, C.-S. Jia, Phys. Lett. A 346 (2005) 54.
[31] H.S. Johnston, J. Heicklen, J. Phys. Chem. 66 (1962) 532.
[32] R.L. Brown, J. Res. Natl. Bur. Stand. 86 (1981) 357.
[33] H.R. Rastegar-Sedehi, Eur. Phys. J. Plus 136 (2021) 514.
[34] C. Tavares, S. Oliveira, V. Fernandes, A. Postnikov, M.I. Vasilevskiy, Softw. Comput. 25 (2021) 6807.
[35] S.K. Tokunaga, J.M. Dyne, E.A. Hinds, M.R. Tarbutt, New J. Phys. 11 (2009) 055038.
[36] C.O. Edet, P.O. Amadi, M.C. Onyeaju, U.S. Okorie, R. Sever, G.J. Rampho, H.Y. Abdullah, I.H. Salih, A.N. Ikot, J. Low Temp. Phys. 202 (2021) 83.
[37] K. Lakaal, M. Kria, J. El Hamdaoui, Varsha, V. Prasad, Vijit V. Nautiyal, M. El-Yadri, L.M. Pérez, D. Laroze, E. Feddi, J. Magn. Magn. Mater. 551 (2022) 169042.
[38] A.N. Ikot, C.O. Edet, P.O. Amadi, U.S. Okorie, G.J. Rampho, H.Y. Abdullah, Eur. Phys. J. D 74 (2020) 1.
[39] C.O. Edet, A.N. Ikot, Eur. Phys. J. Plus 136 (2021) 1.
[40] A.N. Ikot, U.S. Okorie, G. Osobonye, P.O. Amadi, C.O. Edet, M.J. Sithole, G.J. Rampho, R. Sever, Heliyon 6 (2020) e03738.
[41] O. Negrete, F. Peña, P. Vargas, Entropy 20 (2018) 888.
[42] C.O. Edet, A.N. Ikot, U.S. Okorie, G.J. Rampho, M. Ramantswana, R. Horchani, H. Abdullah, J.A. Vinasco, C.A. Duque, A.-H. Abdel-Aty, Int. J. Thermophys. 42 (2021) 138.
[43] R. Khordad, M.M. Mirhosseini, B. Mirhosseini, Iran. J. Sci. Technol. Trans. Sci. 42 (2018) 2355.
[44] R. Khordad, B. Vaseghi, Int. J. Quantum Chem. 119 (2019) e25994.
[45] S.M. Ikhdair, B.J. Falaye, M. Hamzavi, Ann. Physics 353 (2015) 282.
[46] C.O. Edet, A.N. Ikot, M.C. Onyeaju, U.S. Okorie, G.J. Rampho, M.L. Lekala, S. Kaya, Phys. E Low-Dimens. Syst. Nanostruct. 131 (2021) 114710.
[47] C.O. Edet, A.N. Ikot, Mol. Phys. 119 (2021) e1957170.
[48] M. Eshghi, H. Mehraban, Eur. Phys. J. Plus 132 (2017) 1.
[49] H. Hassanabadi, B.H. Yazarloo, A.N. Ikot, N. Salehi, S. Zarrinkamr, Indian J. Phys. 87 (2013) 1219.
[50] S. Flugge, Practical Quantum Mechanics, Springer Science & Business Media, 2012.
[51] N.N. Lebedev, Special Functions and their Applications, in: Chapter 5 (Translated by Richard A. Silverman), Dover Publication, Inc, New York, 1972.
[52] M. R.Setare, E. Karimi, Internat. J. Theoret. Phys. 46 (2007) 1381.
[53] S.H. Dong, Factorization Method in Quantum Mechanics, Springer, Amsterdam, 2007, pp. 150–155.
[54] C.-S. Jia, R. Zeng, X.-L. Peng, L.-H. Zhang, Y.-L. Zhao, Chem. Eng. Sci. 190 (2018) 1.
[55] J. Wang, C.-S. Jia, C.-J. Li, X.-L. Peng, L.-H. Zhang, J.-Y. Liu, ACS Omega 4 (2019) 19193.
[56] C.O. Edet, P.O. Nwbabuzor, E.B. Ettah, C.A. Duque, N. Ali, A.N. Ikot, S. Mahmoud, M. Asjad, Results Phys. 39 (2022) 105749.
[57] C.O. Edet, P.O. Amadi, E.B. Ettah, N. Ali, M. Asjad, A.N. Ikot, Mol. Phys. 120 (2022) e2059025.